Enhanced optoelectronic properties of magnetron sputtered ITO/Ag/ITO multilayers by electro-annealing

(iD) **Zemzem Uyanik,** (iD) **Fulya Turkoglu,** (iD) **Hasan Koseoglu, et al.**

View Online   Export Citation   CrossMark

ARTICLES YOU MAY BE INTERESTED IN

Hollow cathode enhanced capacitively coupled plasmas in $Ar/N_2/H_2$ mixtures and implications for plasma enhanced ALD
Journal of Vacuum Science & Technology B **40**, 044002 (2022); https://doi.org/10.1116/6.0001840

On modeling the induced charge in density-functional calculations for field emitters
Journal of Vacuum Science & Technology B **40**, 042802 (2022); https://doi.org/10.1116/6.0001886

(); https://doi.org/10.1063/PT.6.4.20220630d

Enhanced optoelectronic properties of magnetron sputtered ITO/Ag/ITO multilayers by electro-annealing

Zemzem Uyanik,[1] (iD) Fulya Turkoglu,[1,2,a)] (iD) Hasan Koseoglu,[1,3] (iD) Merve Ekmekcioglu,[1,4]
Bengu Ata,[1] Yasemin Demirhan,[1] (iD) Mehtap Ozdemir,[4] (iD) Gulnur Aygun,[1] (iD) and Lutfi Ozyuzer[1,4] (iD)

AFFILIATIONS

[1]Department of Physics, Izmir Institute of Technology, 35430 Urla, Izmir, Turkey
[2]Department of Metallurgical and Materials Engineering, Iskenderun Technical University, 31200 Iskenderun, Hatay, Turkey
[3]ISTE Center for Science and Technology Studies and Research (ISTE-CSTSR), Iskenderun Technical University, 31200 Iskenderun, Hatay, Turkey
[4]Teknoma Technological Materials Ltd. IZTEKGEB, IZTECH Campus, 35430 Urla, Izmir, Turkey

[a)]Author to whom correspondence should be addressed: fulya.koseoglu@iste.edu.tr

ABSTRACT

Indium tin oxide/silver/indium tin oxide (ITO/Ag/ITO) multilayers have attracted much attention to fulfill the growing need for high-performance transparent conducting oxide electrodes. To make these transparent multilayers work better, electro-annealing, which is a method of self-heating by electric current, can be effective. Moreover, the effect of current on ITO/Ag/ITO multilayers should be investigated to make sure that electronic devices will be reliable over their lifetime. In this study, ITO/Ag/ITO multilayer electrodes with varying Ag thicknesses were grown by DC magnetron sputtering at room temperature. Structural, optical, and electrical properties of these multilayers were investigated before and after electro-annealing. Measurement results revealed that improved optical transmittance and sheet resistance can be obtained by the optimization of Ag thickness for the as-grown ITO/Ag/ITO layers. The highest figure of merit (FoM) value of $17.37 \times 10^{-3}\,\Omega^{-1}$ with optical transmittance of 85.15% in the visible region and sheet resistance of $11.54\,\Omega/\square$ was obtained for the Ag thickness of 16.5 nm for as-grown samples. The electro-annealing of as-grown ITO/Ag/ITO multilayers led to improved optical behavior of the multilayer structure over a wide spectral range, especially in the near-infrared range. Electro-annealing also provided an improvement in the crystallinity and sheet resistance of the electrodes. The improvement of the electrical and optical properties of the structure enabled a FoM of $23.07 \times 10^{-3}\,\Omega^{-1}$ with the optical transmittance of 86.80% in the visible region and sheet resistance of $10.52\,\Omega/\square$. The findings of this work provide proper knowledge of the properties of ITO/Ag/ITO multilayers under electrical current and suggest that the overall performance of the multilayers can be improved by the electro-annealing process.

I. INTRODUCTION

Transparent conducting oxides (TCOs) are used in a variety of applications such as smart windows, organic light-emitting diodes, solar cells, transparent electrodes in LCDs, photodetectors, and IR-reflective coatings.[1–5] Due to its high optical transmittance in the visible region and low resistivity, indium tin oxide (ITO) leads the field over other wide bandgap TCOs such as Al-doped zinc oxide (AZO), Nb-doped titanium dioxide, and Ga-doped zinc oxide (GZO).[6]

Most TCOs require a heat treatment exceeding 300 °C to attain low resistivity and high transmission in the visible region.[7,8] The strengthening of electrical characteristics of ITO thin films by heat treatment is attributed to the elimination of localized electron traps via crystallization as well as an enhancement in charge-carrier concentration.[7] The increase in optical transmittance of the ITO thin films by heat treatment can be attributed to the increase in structural homogeneity and crystallinity.[8] This high-temperature necessity can degrade the performance of organic devices and

deform plastic substrates.[6,9,10] Multilayer TCOs have been studied extensively in recent decades as one of the promising candidates to overcome such issues. The utilization of TCO/metal/TCO multilayer structures was proven to be one of the most effective strategies to improve the electrical and optical properties of TCOs.[11] Metals such as Au, Ag, Al, Cu, and their alloys have been widely explored as an intermediate layer to improve electrical conductivity without disrupting the transparency of the semiconductor material.[12] To increase the performance of these structures, a significant number of TCOs has been explored, including ITO,[7,10,12–15] ZnO,[16] AZO,[17–19] magnesium zinc oxide (MgZnO),[20] fluorine-doped tin oxide (FTO),[21] and tungsten trioxide (WO_3).[22] By optimizing these structures, a selective transparent effect can be obtained in the visible region by suppressing reflection from the metal layer.[23]

ITO/metal/ITO multilayers structures have gained a lot of interest to fulfill the growing need for high-performance TCO electrodes. For these multilayer structures, interlayers such as Au, Ag, and Cu have recently been stated to have a transmittance of more than 87% and sheet resistance of less than $10\,\Omega/\square$.[7,10,12–15,24,25] In comparison with other intermediate layers, Ag is expected to be a superior candidate for developing advanced electrodes due to its low absorption coefficient in the visible region and excellent conductivity.[25] The optical bandgap of ITO/Ag/ITO multilayer (~4.2 eV) was found to be greater than that of ITO thin film (~3.8 eV).[7] According to the optical nonlinearity measurement performed by the Z-scan experiment, it was observed that both the nonlinear refractive index and the nonlinear absorption coefficient for the ITO/Ag/ITO multilayers are much higher than a single ITO layer.[26] Highest Haacke figure of merit (FoM) value of $120.8 \times 10^{-3}\,\Omega^{-1}$ was achieved for the ITO/Ag/ITO structure showing the extraordinary ability of this electrode.[27] Deposition conditions and thicknesses of ITO and Ag thin films have a major impact on the electrical and optical characteristics of ITO/Ag/ITO electrodes. Regarding the intermediate metallic layer, detrimental effects are encountered as the thickness of the metal layer is below 10 nm due to discontinuity of the metallic layer.[28]

Several investigations have emphasized the importance of annealing to improve the quality and homogeneity of the thin films by modifying the deposited layers more efficiently. The effect of annealing on the performance of multilayer structures has also been investigated.[7,29–31] Liu et al. showed that annealing temperature strongly affects the structural, electrical, and optical properties of the magnetron sputtered $SnO_2/Ag/SnO_2$ nano-multilayer structures.[29] Multilayer annealed at 200 °C illustrated a maximum FOM value of $3.39 \times 10^{-2}\,\Omega$ with 91% transmittance and $4.4\,\Omega/\square$ sheet resistance. Chu et al. investigated the effect of annealing temperature and annealing atmosphere on the properties of AZO/Au/AZO multilayers.[30] At an annealing temperature of 200 °C in a vacuum atmosphere, a multilayer having a resistivity of $6.34 \times 10^{-5}\,\Omega$ and transmittance of 92.3% was achieved. Lee et al. obtained a maximum FOM of $106 \times 10^{-3}\,\Omega^{-1}$ for the ITO/Ag/ITO multilayers annealed at 600 °C in N_2.[27] For ITO/Ag/ITO multilayers, the effect of annealing temperature and multilayer geometry was also investigated.[31] An excellent FoM of $120.8 \times 10^{-3}\,\Omega^{-1}$ was obtained for the electrode annealed at 600 °C. Lee et al. showed that the bandgap of the ITO/Ag/ITO electrode increased (~4.5 eV) with annealing up to a temperature of 500 °C.[7] As an alternative to thermal annealing,

electro-annealing, which is a method of self-heating by electric current, was shown to boost the performance of ITO thin films.[32–34] As compared to thermal annealing, thermal budget and kinetic exponent of crystallization of ITO films are significantly reduced after electro-annealing.[32] Electro-annealing has some benefits, including the elimination of the need for an external heater during annealing, and the reduction in heat overloading by the surrounding components due to the direct Joule heat produced by the applied electric field to the film.[32] Furthermore, electro-annealing is appropriate for heat-sensitive substrates[33] since, unlike thermal annealing, crystallization begins and progresses quicker at smaller power levels in the case of electro-annealing due to the effective energy coupling from Joule heating. However, to the best of our knowledge, the effect of electro-annealing on the performance of ITO/Ag/ITO multilayers is still lacking.

ITO/Ag/ITO multilayers have been found to be potential candidates in a variety of electronic devices such as solar cells,[35–37] touch screens,[38] OLEDs,[39] electrochromic devices,[40] etc. The heat generated by the current in electronic devices may change the intrinsic properties of ITO/Ag/ITO multilayers, and their behavior may change significantly. The electronic device no longer behaves in the way it was designed to and may even fail. Therefore, the effect of current on ITO/Ag/ITO multilayers should be investigated to make sure that electronic devices will be reliable over their lifetime.

In this work, ITO/Ag/ITO multilayers having different Ag thicknesses were grown by DC magnetron sputtering on borosilicate glasses at room temperature. The magnetron sputtering technique, which is a type of physical vapor deposition (PVD), has a number of advantages, including excellent uniformity in manufactured thin films, great adherence to substrates, the capability to deposit large areas, a high film growth rate, and the ability to adjust film thickness easily.[6] The objective of this research is to build a proper knowledge of the properties of ITO/Ag/ITO electrodes under electrical current. Therefore, the effect of electro-annealing on the structural, optical, and electrical properties of as-grown ITO/Ag/ITO multilayer films with varying Ag thicknesses has been investigated in this study.

II. EXPERIMENT

Indium tin oxide/Ag/indium tin oxide (ITO/Ag/ITO) multilayers were deposited onto borosilicate glasses by DC magnetron sputtering from 2-in. targets of ITO (Lesker, 99.99% pure with 10 and 90 wt. %, respectively, for SnO_2 and In_2O_3) and Ag (Lesker, purity of 99.99%) at room temperature (RT). In this study, borosilicate was preferred as the substrate since the SLG substrate is broken due to thermal shock when high currents are applied during electro-annealing. In an ultrasonic bath, the substrates were cleaned in the following order: acetone (Merck), alcohol (Merck), and de-ionized water for 10 min each. Moreover, plasma etching was performed for 10 min to eliminate any remaining organic residue. Before thin-film depositions, target surfaces were pre-sputtered for 5 min to prevent the contamination of ITO and Ag thin films. Depositions were carried out with a DC power of 15 W and Ar gas flow of 40 SCCM for both ITO and Ag thin films. The operating pressure for the depositions was between 0.4 and 0.666 kPa. The

distance between the targets and substrate holder was 7.2 cm. Using rotational feedthrough, the sample holder was rotated to deposit ITO, Ag, and ITO thin films onto the borosilicate glasses, respectively. While the deposition durations of ITO thin films were kept constant for 7 min, Ag deposition durations were varied as 13, 15, 17, and 19 s. After ITO/Ag/ITO multilayers were fabricated, electro-annealed was performed in the air by applying current to multilayers. To apply current using an external power supply, copper plates of 1 μm thick, 5 mm wide, and 3 cm in length were mounted to the two opposing edges of the substrates. The k-type thermocouple was used to measure the temperature of the multi-layers. A schematic of the electro-annealing process can be found in Ref. 34. The applied voltages to multilayers were gradually increased every 20 min for 20, 40, and 60 V for a total 1-h electro-annealing process.

The thicknesses of fabricated Ag and ITO thin films were measured with A Veeco DEKTAK 150 profilometer. We obtained multilayers having top and bottom ITO thicknesses of 51.5 nm for the deposition duration of 7 min and Ag thicknesses of 10.5, 12.5, 15, and 16.5 nm for the deposition durations of 13, 15, 17, and 19 s, respectively. To get information about crystal structures of the ITO/Ag/ITO multilayers, x-ray diffraction (XRD) was performed in the Bragg–Brentano focusing geometry on a Phillips X'Pert Pro x-ray diffractometry, with Cu K_α radiation ($\lambda = 1.5406$ Å). XRD patterns were obtained for 2θ values with a step size of 0.016° from 10° to 80° for all samples. Optical properties of ITO/Ag/ITO multi-layers were investigated by transmittance measurements in the wavelength range of 200–2600 nm using a PerkinElmer Lambda 950 UV/VIS/NIR spectrophotometer. Electrical characteristics of ITO/Ag/ITO multilayers were investigated by four-point probe technique using Keithley 2420 source meter.

III. RESULTS AND DISCUSSION

A. Structural analyses

Figure 1 illustrates the x-ray diffraction (XRD) patterns for as-grown and electro-annealed indium tin oxide/silver/indium tin oxide (ITO/Ag/ITO) multilayers having different Ag thicknesses. Since the thicknesses of ITO thin-film layers were kept constant at 51.5 nm, only Ag thicknesses were given in the figures as a legend. XRD patterns of the as-grown ITO/Ag/ITO multilayers exhibit a peak approximately at 34.7° which belongs to (400) reflection from the bixbyite structure of ITO (JCPDS File No. 89-4596). Since the ITO thin films deposited at RT lack the activation energy for Sn to substitute at In sites, many of the Sn^{+2} cations sit as an interstitial ion in the films leading to a higher interplanar spacing. As a result, according to Bragg's law, 2θ moves to lower values. For as-grown multilayers, it can be noticed that as the Ag thickness increases, (400) reflection of the ITO reflection peak gets bigger since incre-ment in the Ag layer improves the crystallinity of the upper ITO layer by acting as a crystalline substrate, which is also in agreement with the number of previously published works.[12,15] The XRD pat-terns of electro-annealed multilayers exhibit characteristics peaks of ITO along (211), (222), (400), (411), (440), and (622) crystallo-graphic directions at 2θ values of 21.62°, 30.80°, 35.68°, 38.21°, 51.41°, and 61.11°, respectively (JCPDS File No. 89-4596). Since tin atoms are fully miscible in the In_2O_3 lattice, none of the
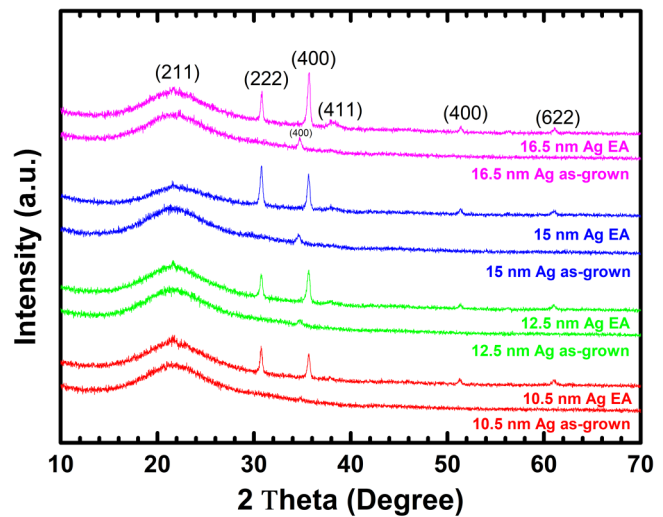

FIG. 1. X-ray diffraction patterns for as-grown and electro-annealed (EA) ITO/Ag/ITO multilayers having 10.5, 12.5, 15, and 16.5 nm Ag thicknesses.

diffractograms display any typical peaks related to Sn, SnO, or SnO_2. As it can be seen from Fig. 1, since the temperature of the multilayers rises as the electrical current flows through them, electro-annealing allows for efficient modification of the ITO thin films and crystallinity improvement. Furthermore, crystalline struc-tures improve in perfection with increasing Ag thickness since the temperature of the multilayer rises more with the thicker Ag layer, as discussed below.

It is also observed that all electro-annealed multilayers have strong (222) and (400) planes which imply the coexistence of $\langle 100 \rangle$ and $\langle 111 \rangle$ textures. While the close-packed (222) plane does not handle oxygen vacancies efficiently in the In_2O_3 body-centered cubic structure, the (400) plane does. As a result, rather than the (222) plane, the sheet resistance of ITO films is determined by the orientation of the (400) plane. As it can be seen from Fig. 1, electro-annealed multilayers become more oriented along the (400) plane as Ag thickness increases. This orientation also reveals why the electro-annealed multilayers' sheet resistance lowers as the Ag thickness increases.

B. Optical analyses

Figure 2 illustrates the optical transmittance spectra of as-grown and electro-annealed ITO/Ag/ITO multilayers having dif-ferent Ag thicknesses in the range of 200–2600 nm. It can be seen that optical transmittance of the multilayers in the visible region (450–650 nm) critically depends on the thicknesses of the Ag layers and electro-annealing. In the case of the varied Ag thicknesses [Fig. 2(a)], increasing Ag thickness results in an increase in trans-mittance in the visible region due to the interference effect caused by Ag intermediate layers.[12,25] The highest average transmittance of 85.94% for the Ag thickness of 15 nm and the lowest average trans-mittance of 74.20% for the Ag thickness of 10.5 nm were obtained.
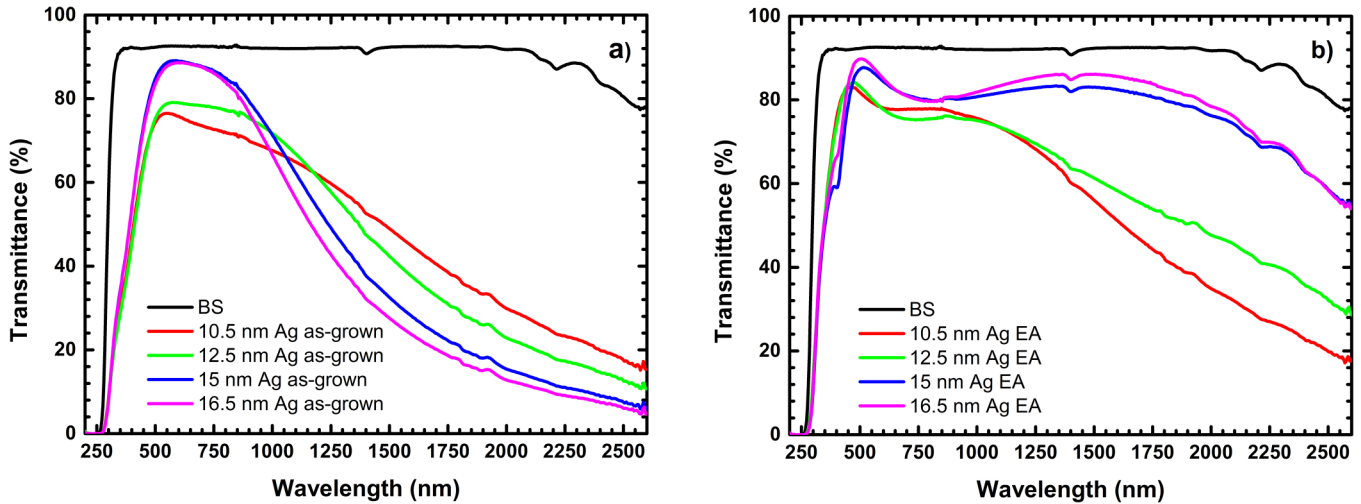
FIG. 2. Optical transmittance spectra (200–2600 nm) of the (a) as-grown and (b) electro-annealed (EA) ITO/Ag/ITO multilayers having 10.5, 12.5, 15, and 16.5 nm Ag thicknesses.

Further increment of Ag thickness to 16.5 nm resulted in slightly lower transparency in the visible region due to the reflection effect. According to several studies, unconnected metal islands caused by low intermediate layer thickness create high sheet resistance and low optical transmittance because of strong scattering from these islands.[28] Optical analysis indicated continuous film formation with the best transmittance and lowest scattering in the visible region obtained with 15 nm Ag thickness. In the near-infrared region (NIR), with increasing Ag intermediate layer thickness, the optical transmittance of the multilayers decreases linearly (more visible above 1300 nm) and shifts to lower wavelengths with the transparent region shrinking. In the NIR, this shift and reduction in transmittance mainly result from the increase in reflection due to the increment of the plasma resonance frequency of the free electron gas with increasing Ag thickness.[12,41] The optical transmittance of multilayers is influenced by the concentration of free carriers in the NIR.[34] Since carrier concentration increases with increasing Ag thickness, the plasma resonance frequency of the

multilayers can be adjusted suitably. As can be visible from Fig. 2(b) and Table I, the visible transmittance of the films is improved by the electro-annealing method. The average transmittance of the electro-annealed multilayers increases up to 86.80% for an Ag thickness of 16.5 nm. More importantly, the electro-annealed ITO/Ag/ITO multilayers demonstrate the ability to achieve higher transmittance over a wide range of wavelengths. Due to the enhanced structural homogeneity and beneficial antireflection effects provided by the electro-annealing process, the optical properties of the multilayers are upgraded. As ITO/Ag/ITO layers are heated by an electrical current flowing through them, Ag impurities may diffuse inside the film structure, leading to a reduction in the thickness of the Ag layer.[31] Diffusion of Ag impurities could lead to improved optical behavior of the multilayer structure over a wide spectral range, especially in the near-infrared regime. It can be noticed that the optical transmittance losses of as-grown multilayer stack at the near-infrared range caused by the reflection effects can be overcome due to the partial diffusion of Ag impurities by

TABLE I. Optical transmittance (T), sheet resistance (R_s), and figure of merit (FoM) of as-grown and electro-annealed (EA) ITO/Ag/ITO multilayers. The table also includes maximum temperatures (T_{max}) reached for electro-annealed samples.

ITO/Ag/ITO (nm/nm/nm)	T_{avg} (%) (450–650 nm)	R_s (Ω/□)	FoM ($\times 10^{-3}$ Ω^{-1})	T (%) at 1500 nm	T_{max} (°C)
51.5/10.5/51.5 as-grown	74.20	38.95	01.30	48.95	—
51.5/12.5/51.5 as-grown	76.16	25.25	02.60	42.34	—
51.5/15/51.5 as-grown	85.94	13.58	16.18	32.52	—
51.5/16.5/51.5 as-grown	85.15	11.54	17.37	27.56	—
51.5/10.5/51.5 electro-annealed	79.98	24.98	04.29	56.06	163
51.5/12.5/51.5 electro-annealed	80.40	20.20	05.59	61.32	277
51.5/15/51.5 electro-annealed	85.09	13.92	14.30	83.05	300
51.5/16.5/51.5 electro-annealed	86.80	10.52	23.07	86.09	328

electro-annealing. It was also demonstrated that as the Ag thickness increases optical transmittance drastically increases because of electro-annealing. Since the temperature of the structure rises more for the thicker Ag layer, Ag impurity diffusion into the top and bottom ITO thin films enhances and the thickness of intermediate Ag thin film decreases. Therefore, it can be concluded that, as a result of electro-annealing, transparency increases due to the reduction of the reflection resulting from the decrease of the intermediate metallic layer thickness. While the electro-annealed multilayer with the Ag thickness of 16.5 nm exhibits the transmittance of 86.09% at 1500 nm, the as-grown counterpart of this multilayer shows the transmittance of 27.56% at 1500 nm. The electro-annealing method is effective in achieving ITO/Ag/ITO electrodes with better optical properties because optical losses are reduced significantly over a broad spectral range.

C. Electrical analyses

Sheet resistance measurements were carried out for both as-grown and electro-annealed ITO/Ag/ITO multilayers because electrode resistive performance is a significant factor in several optoelectronic devices. Figure 3 illustrates the dependence of the sheet resistance of the as-grown and electro-annealed ITO/Ag/ITO multilayers on the Ag thickness as it can be seen that the sheet resistance of the multilayers continuously decreases with increasing Ag thickness.

The sheet resistance of the ITO/Ag/ITO multilayer can be described using the following equation:

$$\frac{1}{R_S} = \frac{1}{R_{ITO,bottom}} + \frac{1}{R_{Ag,middle}} + \frac{1}{R_{ITO,top}} \simeq \frac{1}{R_{Ag}}. \quad (1)$$

As it can be seen from the equation, the Ag conductivity dominates the entire electrical performance in a typical instance when
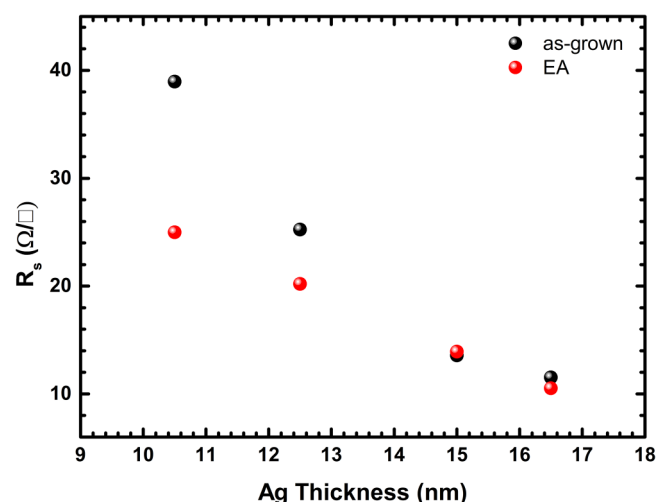

FIG. 3. Sheet resistances (R_s) of the as-grown and electro-annealed (EA) ITO/Ag/ITO multilayers as a function of Ag thicknesses.

an as-grown ITO has a much higher resistivity than Ag. Therefore, the sheet resistance of the as-grown multilayers continuously decreases with increasing Ag thickness.

As it can be seen from Table I, the temperature of the multilayers increases with decreasing sheet resistance of the multilayers. Since the electro-annealing voltage was kept constant, reduced sheet resistance leads to an increment of current flow through multilayers. The temperature of the multilayers increases due to Joule heating. The highest temperatures for electro-annealed ITO/Ag/ITO multilayers were about 163, 277, 300, and 328 °C for the Ag thicknesses of 10.5, 12.5, 15, and 16.5 nm, respectively. R_s values of electro-annealed ITO/Ag/ITO multilayers are lower than as-grown multilayers, where the electro-annealed multilayer with the Ag thickness of 16.5 nm has the least sheet resistance value of 10.52 Ω/□. It can also be noticed from Fig. 3 that as the thickness of Ag increases, the difference between the sheet resistance values of as-grown and electro-annealed ITO/Ag/ITO multilayers reduces. The possible reasons for the obtained results can be explained as follows. As the temperature of the multilayers rises due to the electrical current, Ag impurities can diffuse through the ITO films. The resistance of the single bottom ITO, Ag, and top ITO thin films coupled in parallel results in the overall resistance of the multilayer.[42] Since the partial diffusion of Ag enhances the electrical conductivity of bottom and top ITO thin films, the total resistance of the multilayers decreases. However, since the temperature increases more for the multilayers having thicker Ag intermediate layer, Ag impurity diffusion into the top and bottom ITO layers increases, and accordingly, the thickness of the intermediate layer decrease. Therefore, the electrode resistance is similar for both as-grown and electro-annealed ITO/Ag/ITO multilayers having a thicker Ag layer. Moreover, the conductive behavior of the multilayers can also be described by oxygen vacancies. The number of oxygen vacancies in ITO thin films has a significant influence on sheet resistance.[43] Ionization of oxygen vacancies produces a maximum of two free electrons per vacancy at the donor level, resulting in an enhancement of conductivity. For the electro-annealed ITO/Ag/ITO layers having a thinner Ag intermediate layer (i.e., 10.5 nm), R_s of the electro-annealed multilayers are much lower than that of as-grown multilayers since the low temperature (about 150 °C) enhances the interaction of oxygen atoms with In atoms, resulting in the formation of the In_2O_{3-x} phase is produced.[34] The concentration of oxygen vacancies increases as a result of this formation and R_s decreases more. For electro-annealed ITO/Ag/ITO having a thicker Ag intermediate layer (16.5 nm), the remaining oxygen atoms within the film or on the top surface interact with In atoms and In_2O_{3-x} phase at a high temperature of about 328 °C, resulting from the formation of the In_2O_3 phase. Oxygen vacancy concentration decreases due to this formation and resistance of the ITO films tends to increase.[34] On the other hand, diffusion of Ag impurities into the ITO thin films provides the reduction of the resistance of the ITO thin films. This may also explain similar conductive behavior of as-grown and electro-annealed ITO/Ag/ITO multilayers having a thicker Ag layer.

D. Figure of merit analyses

TCO thin films require both high optical transmittance and low sheet resistance to function well, but this is not always

attainable. Consequently, it is important to optimize the electrical and optical properties as much as feasible. The quality of as-grown and electro-annealed ITO/Ag/ITO multilayers were determined using the figure of merit (FoM) developed by Haacke[44] using the following formula:

$$\text{FoM} = \frac{T^{10}}{R_s}, \tag{2}$$

where T is the optical transmittance at visible range and R_s is the sheet resistance. Our calculations show that both increasing Ag thickness and electro-annealing lead to an increase in the FoM value (Fig. 4 and Table I). The electro-annealed sample with Ag thickness of 16.5 nm has enabled a maximum FoM of $23.07 \times 10^{-3} \, \Omega^{-1}$ because of the enhancement of the conductive and optical properties of the multilayer. On the other hand, the lowest FoM value of $1.30 \times 10^{-3} \, \Omega^{-1}$ was obtained for the as-grown sample with an Ag thickness of 10.5 nm.

Despite these improvements, the FoM values of the fabricated multilayers are far from the highest values obtained in the literature.[27,31] An excellent FoM values of 106×10^{-3} and $120.8 \times 10^{-3} \, \Omega^{-1}$ were obtained for the multilayers annealed at 600 °C.[27,31] However, as discussed before, high temperatures can degrade the performance of organic devices and deform plastic substrates.[6,9,10] Moreover, high temperatures may prevent these electrodes from being implanted in electronic devices. On the other hand, as discussed before, electro-annealing is appropriate for heat-sensitive substrates.[33] Increasing the FOM values obtained in our study could have been possible by adjusting the geometric parameters of the structure more precisely. Many studies have shown that geometrical variables such as thin-film thicknesses in TCO/metal/TCO structures play a crucial impact in determining electrode performance.[34,45] Many studies have shown that geometrical variables such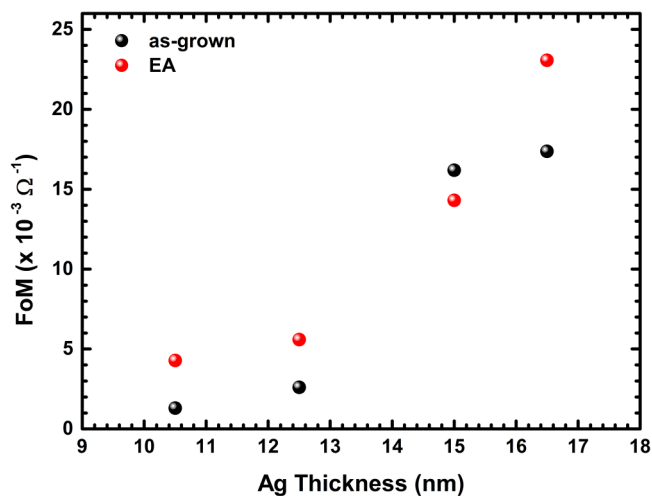 as thin-film thicknesses in TCO/metal/TCO structures play a crucial impact in determining electrode performance. By adjusting the thicknesses of ITO films and varying the position of the Ag layer in multilayers, increased transmittance in the visible region can be attained by controlling interference phenomena, resulting in higher FOM values. However, to prevent the diversification of our work, we only focused on the effects of Ag thickness and electro-annealing in this study. The results of this study provide suitable information on the properties of ITO/Ag/ITO multilayers under electric current and suggest that the overall performance of the multilayers can be improved by the electro-annealing process.

IV. SUMMARY AND CONCLUSIONS

In this study, indium tin oxide/silver/indium tin oxide (ITO/Ag/ITO) multilayers were fabricated by DC magnetron sputtering on borosilicate substrates at room temperature. Understanding the impact of electric current on transparent conducting oxide thin films is crucial for improving the reliability and longevity of electronic devices. Therefore, structural, optical, and electrical properties of ITO/Ag/ITO multilayers fabricated with different Ag thicknesses were investigated before and after the electro-annealing process. The performance of ITO/Ag/ITO multilayers critically depends both on Ag thickness and electro-annealing. Increasing the Ag thickness led to a significant increase in the transmittance in the visible region and decrease in sheet resistance of the samples. The highest figure of merit (FoM) value of $17.37 \times 10^{-3} \, \Omega^{-1}$ was obtained for the Ag thickness of 16.5 nm for as-grown samples. On the other hand, it was observed that the transmittance of the ITO/Ag/ITO multilayers in the near-infrared region decreases linearly and shifts to lower wavelengths with increasing thickness due to the increment of the plasma resonance frequency of the free electron gas with increasing Ag thickness. In the case of electro-annealing of as-grown multilayers, it was shown that the optical transmittance losses in the near-infrared range caused by the reflection effects can be overcome due to partial diffusion of Ag impurities into ITO by electro-annealing. For the multilayer with the 16.5 nm Ag thickness, optical transmittance was increased from 27.56% to 86.09% at 1500 nm by electro-annealing. Electro-annealing also provided an improvement in the crystallinity, optical transmittance in the visible region, and sheet resistance of ITO/Ag/ITO multilayers. Enhancement of the structure's conductive and optical behavior supplied FoM of $23.07 \times 10^{-3} \, \Omega^{-1}$ for the sample with the 16.5 nm Ag thickness. Our findings indicate that a significant reduction of the optical losses over a broad spectral range and reduction of sheet resistance by the electro-annealing process can enable the development of improved optoelectronic and photovoltaic devices.

FIG. 4. Figure of merit (FoM) of the as-grown and electro-annealed (EA) ITO/Ag/ITO multilayers as a function of Ag thicknesses.

AUTHOR DECLARATIONS

Conflict of interest

The authors have no conflicts to disclose.

Author Contributions

Zemzem Uyanik: Investigation (equal). **Fulya Turkoglu:** Investigation (equal); Writing – original draft (equal); Writing – review and editing (equal). **Hasan Koseoglu:** Visualization (equal); Writing – original draft (equal); Writing – review and editing (equal). **Merve Ekmekcioglu:** Investigation (equal). **Bengu Ata:** Investigation (equal). **Yasemin Demirhan:** Formal analysis (equal); Investigation (equal). **Mehtap Ozdemir:** Formal analysis (equal); Resources (equal). **Gulnur Aygun:** Resources (equal); Supervision (equal); Writing – review and editing (equal). **Lutfi Ozyuzer:** Conceptualization (equal); Resources (equal); Supervision (equal); Writing – review and editing (equal).

DATA AVAILABILITY

The data that support the findings of this study are available from the corresponding author upon reasonable request.

REFERENCES

[1] L. Zhao, Z. Zhou, H. Peng, and R. Cui, Appl. Surf. Sci. **252**, 385 (2005).
[2] X. Yu, T. J. Marks, and A. Facchetti, Nat. Mater. **15**, 383 (2016).
[3] T. Yamada, T. Morizane, T. Arimitsu, A. Miyake, H. Makino, N. Yamamoto, and T. Yamamoto, Thin Solid Films **517**, 1027 (2008).
[4] E. H. Ko, H. J. Kim, S. J. Lee, J. H. Lee, and H. K. Kim, RSC Adv. **6**, 46634 (2016).
[5] M. Stolze, D. Gogova, and L. K. Thomas, Thin Solid Films **476**, 185 (2005).
[6] Y. Demirhan, H. Koseoglu, F. Turkoglu, Z. Uyanik, M. Ozdemir, G. Aygun, and L. Ozyuzer, Renew. Energy **146**, 1549 (2020).
[7] J. H. Lee, K. Y. Woo, K. H. Kim, H. D. Kim, and T. G. Kim, Opt. Lett. **38**, 5055 (2013).
[8] T. M. Hammad, Phys. Status Solidi A **206**, 2128 (2009).
[9] F. Turkoglu, H. Koseoglu, S. Zeybek, M. Ozdemir, G. Aygun, and L. Ozyuzer, J. Appl. Phys. **123**, 165104 (2018).
[10] N. Erdogan, F. Erden, A. T. Astarlioglu, M. Ozdemir, S. Ozbay, G. Aygun, and L. Ozyuzer, Curr. Appl. Phys. **20**, 489 (2020).
[11] H. Zhou et al., ACS Appl. Mater. Interfaces **10**, 16160 (2018).
[12] X. Fang, C. L. Mak, J. Dai, K. Li, H. Ye, and C. W. Leung, ACS Appl. Mater. Interfaces **6**, 15743 (2014).
[13] S. Ozbay, N. Erdogan, F. Erden, M. Ekmekcioglu, M. Ozdemir, G. Aygun, and L. Ozyuzer, Appl. Surf. Sci. **529**, 147111 (2020).
[14] M. Chakaroun, B. Lucas, B. Ratier, and M. Aldissi, Energy Procedia **31**, 102 (2012).
[15] D. Kim, Appl. Surf. Sci. **256**, 1774 (2010).
[16] M. Philipp, M. Knupfer, B. Büchner, and H. Gerardin, J. Appl. Phys. **109**, 063710 (2011).
[17] K. H. Choi, Y. Y. Choi, J. A. Jeong, H. K. Kim, and S. Jeon, Electrochem. Solid State Lett. **14**, H152 (2011).
[18] H. K. Park, J. W. Kang, S. I. Na, D. Y. Kim, and H. K. Kim, Sol. Energy Mater. Sol. Cells **93**, 1994 (2009).
[19] T. Dimopoulos, G. Z. Radnoczi, B. Pécz, and H. Brückl, Thin Solid Films **519**, 1470 (2010).
[20] H. J. Lee, J. W. Kang, S. H. Hong, S. H. Song, and S. J. Park, ACS Appl. Mater. Interfaces **8**, 1565 (2016).
[21] S. Yu, L. Li, X. Lyu, and W. Zhang, Sci. Rep. **6**, 20399 (2016).
[22] S. W. Liu, T. H. Su, P. C. Chang, T. H. Yeh, Y. Z. Li, L. J. Huang, H. Y. Chen, and C. F. Lin, Org. Electron. **31**, 240 (2016).
[23] A. Zolanvari, R. Norouzi, and H. Sadeghi, J. Mater. Sci. Mater. Electron. **26**, 4085 (2015).
[24] W. Wei, R. Hong, J. Wang, C. Tao, and D. Zhang, J. Mater. Sci. Technol. **33**, 1107 (2017).
[25] J. A. Jeong, Y. S. Park, and H. K. Kim, J. Appl. Phys. **107**, 023111 (2010).
[26] K. Wu, Z. Wang, J. Yang, and H. Ye, Opt. Lett. **44**, 2490 (2019).
[27] F. Djeffal, H. Ferhati, A. Benhaya, and A. Bendjerad, Superlattice Microstruct. **130**, 361 (2019).
[28] J. T. Guske, J. Brown, A. Welsh, and S. Franzen, Opt. Express **20**, 23215 (2012).
[29] L. Liu, S. Ma, H. Wu, B. Zhu, H. Yang, J. Tang, and X. Zhao, Mater. Lett. **149**, 43 (2015).
[30] C. H. Chu, H. W. Wu, and J. L. Huang, Thin Solid Films **605**, 121 (2016).
[31] S. Y. Lee, Y. S. Park, and T. Y. Seong, J. Alloys Compd. **776**, 960 (2019).
[32] A. Rogozin, N. Shevchenko, M. Vinnichenko, M. Seidel, A. Kolitsch, and W. Möller, Appl. Phys. Let. **89**, 061908 (2006).
[33] D. H. Lee, S. H. Shim, J. S. Choi, and K. B. Yoon, Appl. Surf. Sci. **254**, 4650 (2008).
[34] H. Koseoglu, F. Turkoglu, M. Kurt, M. D. Yaman, F. G. Akca, G. Aygun, and L. Ozyuzer, Vacuum **120**, 8 (2015).
[35] J. A. Jeong and H. K. Kim, Sol. Energy Mater. Sol. Cells **93**, 1801 (2009).
[36] Y. S. Park, H. K. Park, J. A. Jeong, H. K. Kim, K. H. Choi, S. I. Na, and D. Y. Kim, J. Electrochem. Soc. **156**, H588 (2009).
[37] Y. S. Park, K. H. Choi, and H. K. Kim, J. Phys. D: Appl. Phys. **42**, 235109 (2009).
[38] C. C. Wu, RSC Adv. **8**, 11862 (2018).
[39] J. Lewis, S. Grego, B. Chalamala, E. Vick, and D. Temple, Appl. Phys. Lett. **85**, 3450 (2004).
[40] T.-H. Kim, S.-H. Park, D.-H. Kim, Y.-C. Nah, and H.-K. Kim, Sol. Energy Mater. Sol. Cells **160**, 203 (2017).
[41] M. Bender, W. Seelig, C. Daube, H. Frankenberger, B. Ocker, and J. Stollenwerk, Thin Solid Films **326**, 67 (1998).
[42] Y. Y. Choi, K. H. Choi, H. Lee, H. Lee, J. W. Kang, and H. K. Kim, Sol. Energy Mater. Sol. Cells **95**, 1615 (2011).
[43] O. Tuna, Y. Selamet, G. Aygun, and L. Ozyuzer, J. Phys. D: Appl. Phys. **43**, 055402 (2010).
[44] G. Haacke, J. Appl. Phys. **47**, 4086 (1976).
[45] F. Turkoglu, H. Koseoglu, M. Ekmekcioglu, A. Cantas, M. Ozdemir, G. Aygun, and L. Ozyuzer, J. Mater. Sci. Mater. Electron. **33**, 10955 (2022).